Journal of Applied Polymer Science

Design and verification of a single slab RAS through mass production of glass/MWNT added epoxy composite prepreg

Jae-Hwan Shin,[1] Hong-Kyu Jang,[2] Won-Ho Choi,[1] Tae-Hoon Song,[1] Chun-Gon Kim,[1] Woo-Yong Lee[3]

[1]Department of Aerospace Engineering, Korea Advanced Institute of Science, Guseong-dong, Yuseong-gu, Daejeon 305-701, Republic of Korea

[2]Composites Research Center, Korea Institute of Materials Science, 797 Changwondaero, Seongsanggu, Changwon, Gyeongnam 642-831, Korea

[3]The 1st R&D Institute-3, Agency for Defense Development, Daejeon 305-600, Republic of Korea

Correspondence to: C. -G. Kim (E-mail: cgkim@kaist.ac.kr)

ABSTRACT: In this study, glass fiber composite prepreg is manufactured with multi-walled carbon nanotube (MWNT) added epoxy using two different methods. Because MWNT agglomeration occurs, the calendering dispersion method is used to resolve this problem. The tensile and shear tests of glass/MWNT 1.8wt % added epoxy composite (CNT18) are conducted and the results are compared with the properties of a commercial glass/epoxy composite (GEP 118). The complex permittivity is measured using a network analyzer and a waveguide in the Ku-band. A single slab radar absorbing structure (RAS) is also designed and verified. It is found that the tensile and shear properties of CNT18 are sufficient to replace GEP 118 as a structural material. Furthermore, the—10 dB bandwidth and reflection loss of the RAS using CNT18 is 12.87 to 17.78 GHz (4.91 GHz) and—29.2 dB at 14.95 GHz, respectively. The measurement results align well with the simulation results. © 2015 Wiley Periodicals, Inc. J. Appl. Polym. Sci. **2015**, *132*, 42019.

KEYWORDS: composites; dielectric properties; manufacturing; mechanical properties; nanotubes

Received 23 August 2014; accepted 19 January 2015

DOI: 10.1002/app.42019

INTRODUCTION

Until the 20th century, the difficulties in the manufacturing methods and high production costs prevented wide spread use of composite materials. These days, however, the application of composite materials is increasingly common using the modified manufacturing and production methods, as well as lowered material costs.[1]

In particular, carbon fiber reinforced composite materials are widely used in aircraft structures in order to reduce weight and increase fuel efficiency. For example, two of the latest civil aviation aircrafts, i.e. the Boeing B787 and Airbus A350, use carbon fiber reinforced composite materials in more than 50% of the aircraft structures.[2]

Fiber reinforced composite materials have potential for multifunctional applications including radar absorbing structures (RASs). The RASs are not only load bearing structures, but also absorb electromagnetic waves. These features are realized through adding nanofillers to the matrix or through creating periodic patterns using conducting polymers. The RASs is distinguished from EMI shielding. The EMI shielding is used to minimize electrical noise from electric devices and its application targets are internally located electric devices.[3] However, purpose of the RASs is absorbing electromagnetic wave from far field and minimizing reflection.

Much research has manufactured composite materials with nanofiller [e.g. carbon black, carbon nanotubes (CNTs), and carbon nanofibers (CNFs)] and magnetic materials (e.g. ferrite).[3–9] Generally, these studies have been conducted at laboratory specimen scale and the reported products have not been developed to become a massive produced composite prepreg.

A prepreg must be manufactured in order to realize the multifunctional composite structure. Some research has manufactured prepreg using CNT added epoxy.[10] However, the CNTs were dispersed and mixed with the epoxy resin using a mechanical stirring method. Therefore, the prepreg exhibited CNT agglomeration in the matrix.

In this study, the CNT agglomeration in the epoxy resin of the prepreg was resolved using the calendaring dispersion method. Then, prepreg was manufactured using multi-walled carbon nanotube (MWNT) added epoxy resin in the same machine as the general prepreg manufacturing of a hot melt process. Afterwards, the glass/MWNT added epoxy composite prepreg was

cured using an autoclave, and complex permittivity of the composite was measured in the Ku-band (12.4–18 GHz) in order to design a RAS. Finally, a single slab absorber was fabricated and its electromagnetic wave absorption properties were verified.

PREPREG SYSTEM

Materials

The CNTs (CM-95) were manufactured by Hanhwa Chemical, Korea; the CNTs were MWNTs and they were entangled type. The CNTs were synthesized using a catalytic chemical vapor deposition (CVD) process. The carbon purity was >95%. The glass fiber (G118) supplied by Hankuk Fiber, Korea, was used as the reinforcing fabric of the prepreg. The glass fiber was a woven E-glass fiber and its yarn density (count/inch) was 34 in the warp direction and 30 in the fill direction. Two types of liquid epoxy resin (YD-128 and YD-114) were used to produce MWNT added epoxy resin, and a solid epoxy resin (YD-011) was used to manufacture the prepreg. The epoxies and amine hardener were supplied by KUKDO Chemical, Korea.

Prepreg Manufacturing Method

There are two common methods for manufacturing composite prepreg: the solvent dip method and the hot melt method. First, in the solvent dip method, a resin tank filled with the resin solution dissolved by solvent must be prepared and the glass fiber must be passed through the resin tank. Then, the prepreg is finalized via the solvent evaporating in a drying oven. The solvent dip method is simple and it easily manufactures the prepreg. However, during the solvent evaporating process, it is not possible to completely evaporate the solvent. Therefore, during the composite curing using the prepreg manufactured via the solvent dip method, the remaining solvent in the prepreg could generate voids in the composites, and voids degrade the mechanical properties. The solvent dip method is usually used for glass fabric composite prepreg.

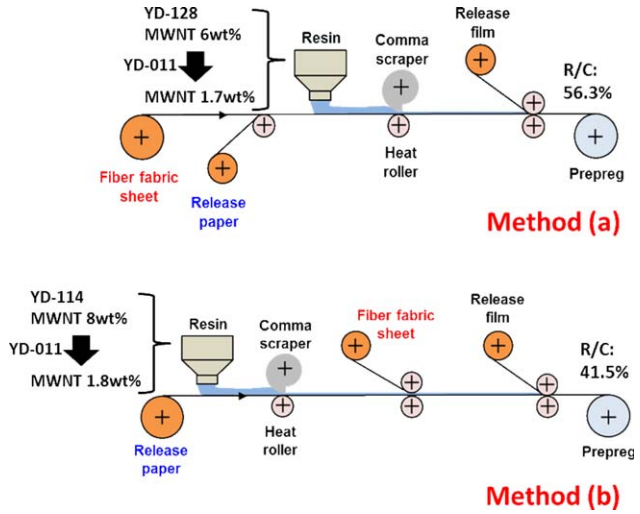

Figure 1. Glass/MWNT added epoxy prepreg manufacturing process. [Color figure can be viewed in the online issue, which is available at wileyonlinelibrary.com.]

The hot melt method does not use solvents. This method requires preparation of resin coated release paper or film, and

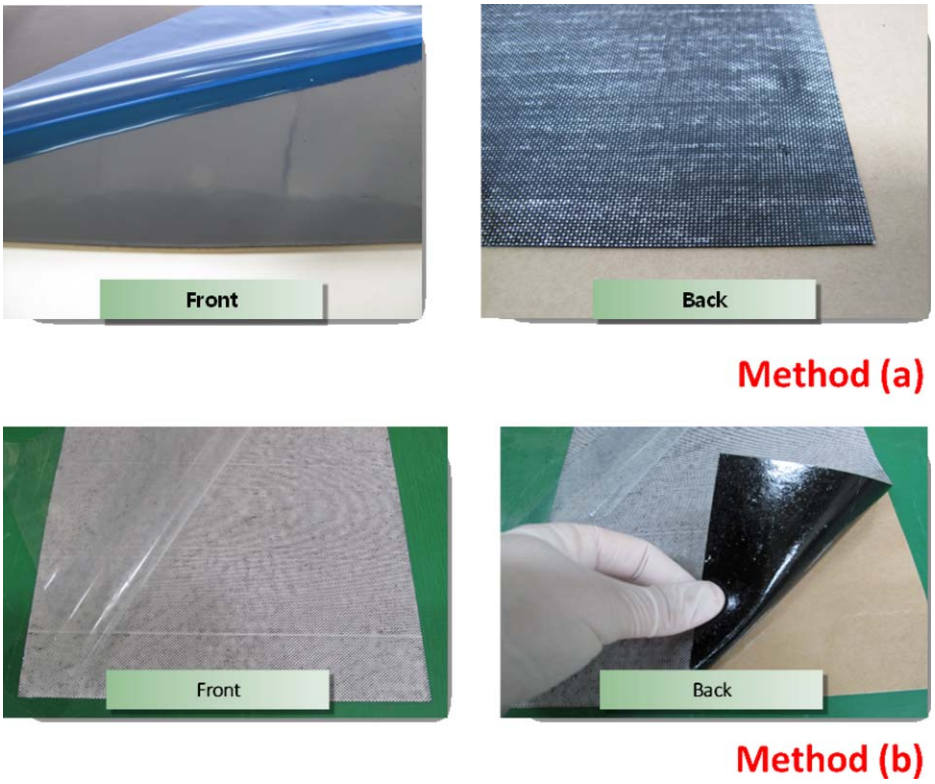

Figure 2. Prepreg surfaces: front surface (left) and back surface (right). [Color figure can be viewed in the online issue, which is available at wileyonlinelibrary.com.]

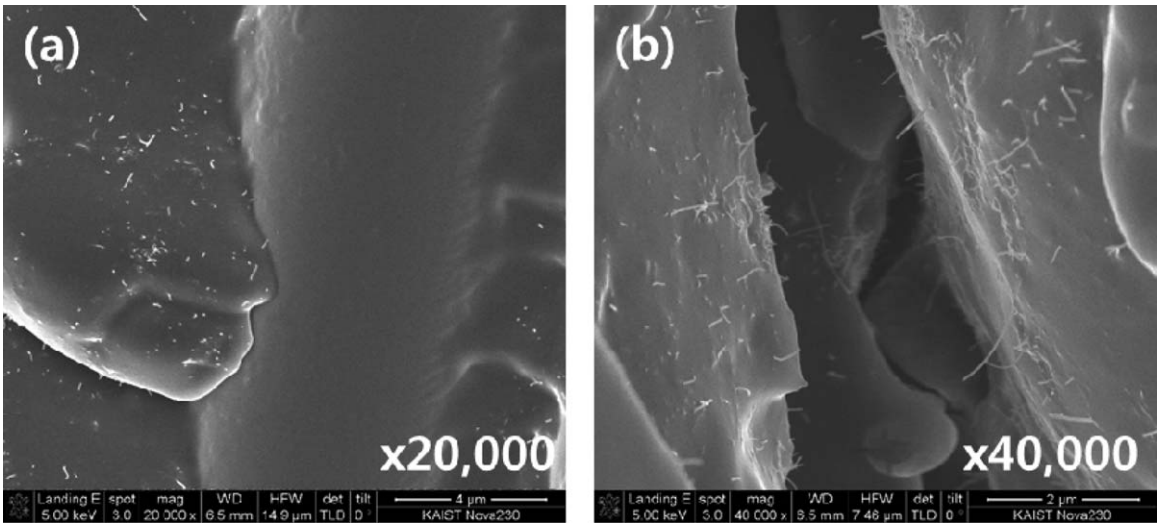

Figure 3. Dispersion states of MWNT in the prepregs; (a) fiber matrix interface and (b) matrix.

then the placement of the reinforcing fiber on the release paper. Then, the release paper with the reinforcing fiber passed through a compressive roller in order to impregnate the fiber with the resin. The hot melt method is usually used to manufacture both unidirectional and fabric prepreg and carbon fiber reinforced prepreg.[11]

The prepreg manufacturing method used in this study differs to the general manufacturing methods described above.

The dispersion method of calendering, which has been investigated in previous research,[7] was applied in order to disperse the MWNTs uniformly in the liquid epoxy. In the previous research, two dispersion methods (homogenizing and calendering methods) were compared.[7] The calendering method exhibited better dispersion results and another study also confirmed that the calendering method is the best method for dispersing micro- and nano-particles.[12] This calendering method is a dispersion method that uses the "three-roll-mill" machine. This dispersion method uses the shear force between two rollers rotating in opposite directions.

However, it is not possible to use the calendering method to directly disperse MWNTs into the prepreg resin because prepreg resin is based on a solid epoxy at room temperature. Therefore, a high weight fraction of MWNTs was dispersed into a liquid epoxy at room temperature using the calendering method; then, using an agitator, the MWNTs were added to the epoxy mixed with a liquefied solid epoxy at 80°C. During the mixing process, the temperature was maintained using a heater in order to prevent the solid epoxy solidifying. The weight fraction of MWNTs in the liquid resin was 6 wt % for YD-128 and 8 wt % for YD-114.

In this study, two different methods were used to manufacture the glass/MWNT added epoxy composite prepreg. In Method (a), using the MWNT added epoxy resin, the resin was applied from a resin tank to the glass fabric and the surplus resin was removed using comma scraper to control the resin content (RC) of the prepreg. In Method (b), the MWNT added epoxy resin was applied from a resin tank to the release paper, and the surplus resin was removed using comma scraper as in Method (a). The characteristics of the prepregs were that the resin applied to the surface exhibited a resin-rich region and the opposite surface exhibited a fibrous dry region. Because the methods did not use solvent, they had the advantage of minimizing voids. However, if sufficient pressure and vacuum were not applied during the prepreg curing, voids could remain in the composite laminate because the resin was only applied to one side when the prepreg was manufactured. The MWNT weight fractions of the prepregs were 1.7 wt % for the Method (a) prepreg and 1.8 wt % for the Method (b) prepreg based on the epoxy resin matrix. There is one type of wt % of MWNT for each manufacturing methods because of the minimum order length of the prepreg was 200 m, so manufacturing various wt % of MWNT added glass epoxy prepreg was difficult. However, the complex permittivity of the MWNT added glass epoxy composite prepreg depending on the wt % of MWNT was confirmed through previous research[7] and several prepreg samples supplied by prepreg manufacturing company, and the wt % of MWNT was decided based on the findings in order to realize RAS. The prepreg manufacturing methods are described in Figure 1, and their configuration is presented in Figure 2. The prepregs exhibited different RC, i.e. the weight ratio between the resin and fiber in the prepreg, because of the different manufacturing methods. The RC of each

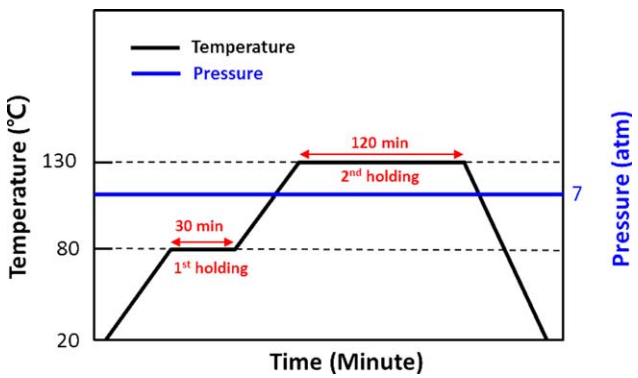

Figure 4. Curing cycle of the prepreg. [Color figure can be viewed in the online issue, which is available at wileyonlinelibrary.com.]

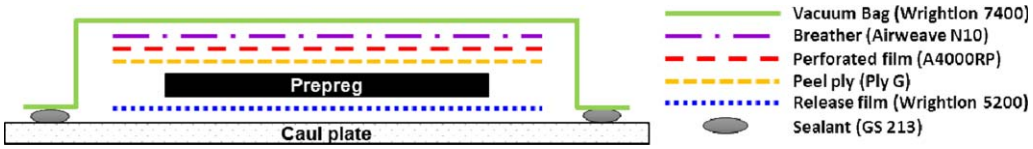

Figure 5. Stacking sequence of vacuum bagging materials and prepreg. [Color figure can be viewed in the online issue, which is available at wileyonlinelibrary.com.]

prepreg was 56.3% for Method (a) and 41.5% for Method (b). The characteristic of each prepreg are summary in Table 1.

The dispersion states of the MWNT in the prepreg were confirmed using a scanning electron microscope (SEM; Nova230, FEI Company, USA). A platinum coating was applied to the prepreg specimen in order to obtain the SEM images. The MWNTs were dispersed evenly and agglomeration was not found, as seen in Figure 3.

Composite Curing Cycle

The composite prepreg used in this study was cured using an autoclave curing process. The curing cycle is illustrated in Figure 4. The first temperature holding was at 80°C for 30 minutes; the second holding was at 130°C for 120 minutes. A pressure of 7 atm and a vacuum bagging method were applied during the curing. The stacking sequence of the vacuum bagging materials and prepreg is presented in Figure 5. The vacuum bagging materials were supplied by Airtech (USA).

Tensile and Shear Test

The specimens were prepared and tested for tensile tests according to ASTM D3039.[13] Emery cloth was used as a tab on both sides of the specimen ends. The tensile test was conducted using a universal test machine (UTM; Instron 4482, Instron, USA) with a 100 kN load cell. A strain gage (FCA-2–11, Tokyo Sokki Kenkyujo, Japan) was attached to the center of the specimen in order to measure strain. The glass/MWNT 1.7 wt % added epoxy composite (CNT17) manufactured using Method (a) and the glass/MWNT 1.8 wt % added epoxy composite (CNT18) manufactured using Method (b) were prepared in the warp direction of the fabric prepreg. The commercial glass fiber/epoxy composite (GEP 118, Muhan Composites, Korea) was also prepared in order to compare the tensile properties. Five specimens were prepared for every test. The tensile modulus was obtained in the 1000–3000 με strain range, and the tensile strength was calculated from the breaking point data.

The shear tests were conducted as described in ASTM D5397.[14] The specimen was prepared as a V-notch specimen with a thickness of 3.5 mm. A 10 kN load cell was used and the same strain gage as that used in the tensile test was used. The three composites (CNT17, CNT18, and GEP 118) were also tested and compared. The shear modulus was calculated from the strain range between 1550 and 5500 με, and the shear strength was determined using 0.2% offset method with a shear modulus line along the strain axis from the origin. Test setup and test specimen are shown in Figure 6.

The fiber volume fraction, which is an important factor in composites, was also measured. It was measured using the matrix burn off muffle furnace method as described in ASTM D2171-09.[15] The fiber volume fraction was achieved through burning off the resin of the composites at 565°C for 6 hours.

Complex Permittivity and Reflection Loss Measurement

The complex permittivities of the CNT17 and CNT18 composites were measured in order to design an electromagnetic wave

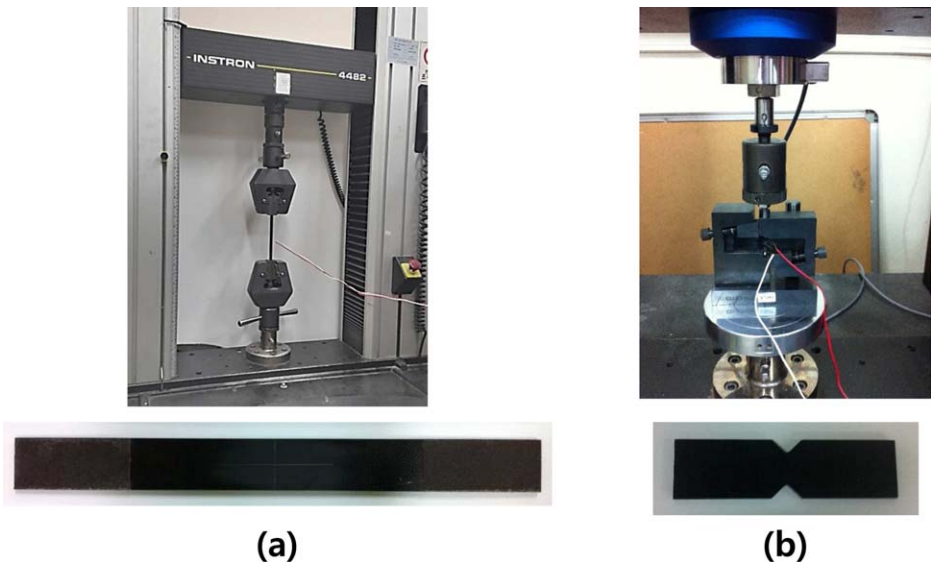

Figure 6. Test setup and test specimen; (a) Tensile test and (b) Shear test [Color figure can be viewed in the online issue, which is available at wileyonlinelibrary.com.]

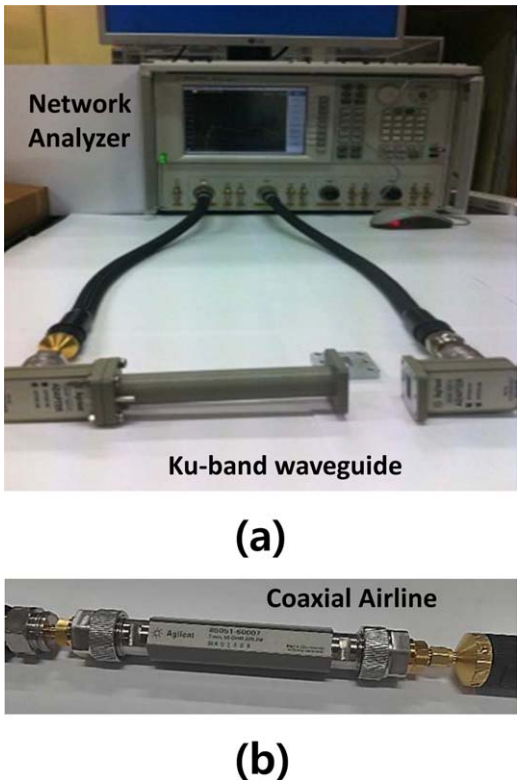

Figure 7. (a) Complex permittivity measurement setup and (b) reflection loss measurement setup. [Color figure can be viewed in the online issue, which is available at wileyonlinelibrary.com.]

absorber. A diamond cutter was used to cut the composites for the measurement.

A network analyzer (N5230C), rectangular waveguide (P11644A WR-62), airline (7 mm, 50 ohm; 85051-60007), and economy calibration kit (7 mm; 85050D) manufactured by Agilent Technologies shown in Figure 7 were used to measure the S-parameters. The complex permittivity was calculated using an Agilent 85071 commercial program. The complex permittivity was measured in Ku-band (12.4–18 GHz) using a rectangular waveguide and cross section of the specimen was 15.8 x 7.9 mm^2. The reflection loss was measured in the Ku-band using a coaxial airline and a donut-shape specimen was prepared. The specimen's outer diameter was 7 mm and its inner diameter was 3.04 mm. The specimen's tolerance limit was −0.02 mm for the rectangular waveguide, and −0.02 mm (outer diameter) and +0.02 mm (inner diameter) for the coaxial airline.

Design Single Slab Absorber

In this article, the RAS is a single slab. A single slab absorber can be considered a transmission line equivalent circuit as depicted in Figure 8. This transmission line equivalent circuit consists of the characteristic impedance (Z) of each layer, which is expressed as in the following equation:

$$Z_{\text{in}} = Z_c \frac{Z_L + Z_c \tanh(\gamma_c \text{d})}{Z_C + Z_L \tanh(\gamma_c \text{d})} \quad (1)$$

$$Z_c = Z_0 \sqrt{\frac{\mu_r}{\varepsilon_r}}, \gamma_c = j\frac{2\pi}{\lambda}\sqrt{\varepsilon_r \mu_r} \quad (2)$$

where γ_c is the propagation constant, d is the absorber thickness, ε_r is the relative complex permittivity, μ_r is the relative complex permeability, and λ is the wavelength of the target frequency.

Applying the conditions of the characteristic impedance of the metal ($Z_L = 0$) and a dielectric lossy material ($\mu_r = 1$), and substituting eq. (2) into eq. (1), the equation of nonreflecting condition ($Z_{in} = Z_0$) is derived as described in eq. (3). If the frequency and complex permittivity are given, the matching thickness (d) can be determined using eq. (3).[16]

$$1 = \frac{1}{\sqrt{\varepsilon_r}} \tanh\left(j\frac{2\pi d}{\lambda}\sqrt{\varepsilon_r}\right) \quad (3)$$

The solution sets of the eq. (3) were obtained using MATLAB. In-house code was used to determine the solution sets. The target frequency, the center frequency of the Ku-band (15 GHz), was selected.

RESULTS AND DISCUSSION

Tensile and Shear Tests

The tensile test and shear test results are presented in Figures 9 and 10, respectively. The tensile properties of CNT17 were lower than those of CNT18. These results can be explained by the fiber volume fraction (v_f) of the composites as detailed in Figures 9 and 10. Because CNT18 had a lower RC than CNT17, this led to a difference in the fiber volume fraction. The surplus resin in the prepregs was removed during the curing process in the autoclave, but it was limited and could not remove all surplus resin. Therefore, the higher RC caused a lower fiber volume fraction and it consequently had lower tensile properties. CNT18 exhibited almost the same tensile modulus as GEP 118 and a higher tensile strength than GEP 118.

The shear test results indicate the same trend as the tensile test results. CNT17 exhibited the lowest shear modulus and strength, and GEP 118 exhibited the highest values. This can

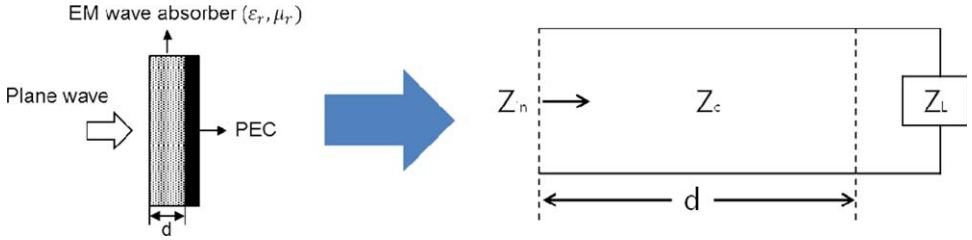

Figure 8. Schematic design of single slab electromagnetic wave absorber (left) and transmission line equivalent circuit (right). [Color figure can be viewed in the online issue, which is available at wileyonlinelibrary.com.]

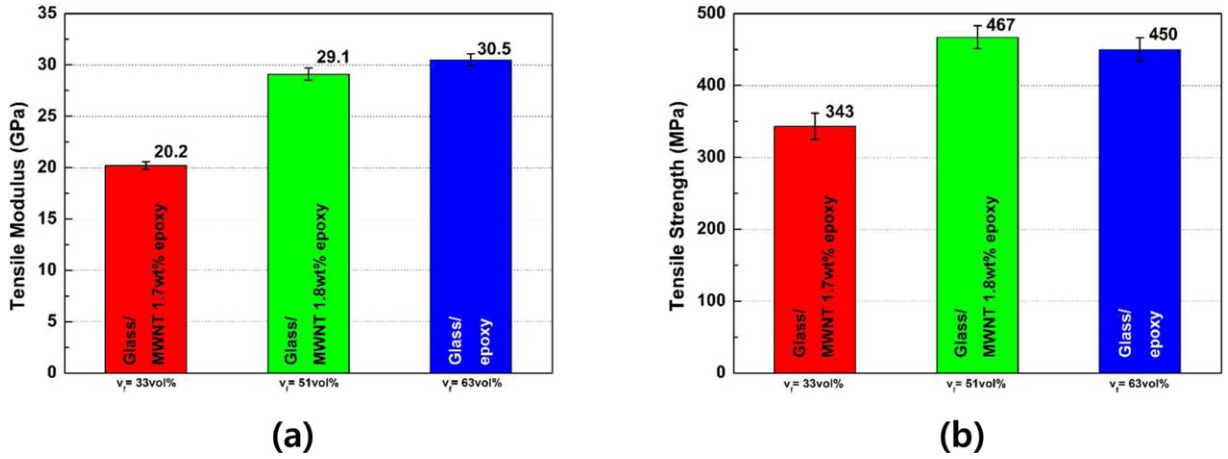

Figure 9. Tensile test results: (a) Modulus, (b) Strength. [Color figure can be viewed in the online issue, which is available at wileyonlinelibrary.com.]

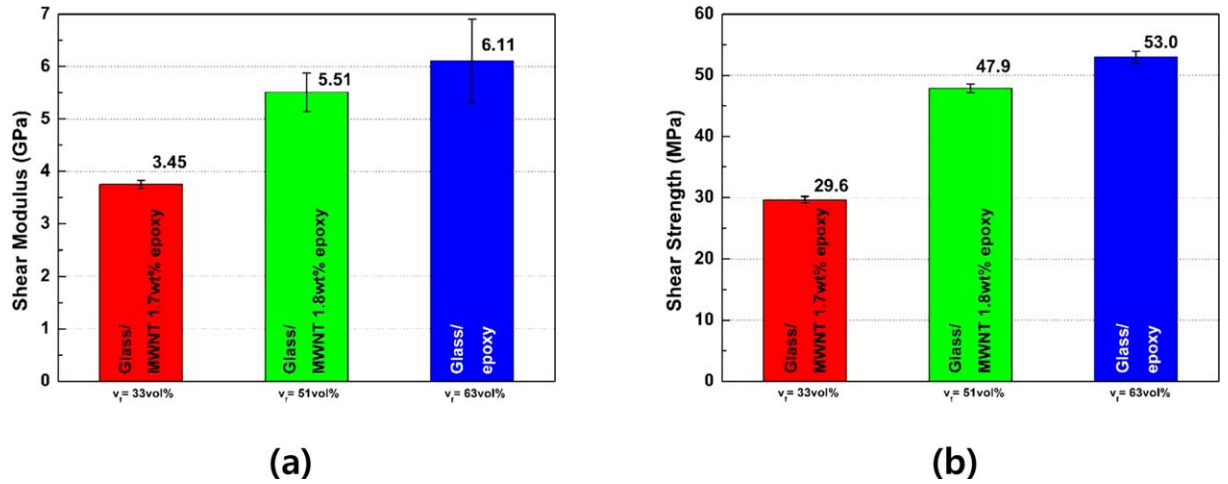

Figure 10. Shear test results: (a) Modulus, (b) Strength. [Color figure can be viewed in the online issue, which is available at wileyonlinelibrary.com.]

be explained through the fiber volume fraction of the composites; the fiber volume fraction effect is clearer than the tensile test results because the shear properties are followed by the inverse rule of the mixture. The inverse rule of the mixture is more sensitive than the rule of mixture toward the fiber volume fraction. In Table II, the tensile and shear test results were normalized by the fiber volume fraction of the prepregs. CNT17 and CNT18 showed similar values. This means that the fiber volume fraction is the main factor behind the tensile and shear properties. Consequentially, the manufacturing Method (b) is more effective than Method (a) from a mechanical point of view.

Complex Permittivity and Single Slab Absorber

The complex permittivities of the three composites were measured using the network analyzer and the waveguide system described previously. The measurement results are illustrated in Figure 11. GEP 118 had the lowest complex permittivity. The glass/MWNT-added epoxy composites had higher complex permittivities than GEP 118 because complex permittivity is controlled by the MWNT weight fraction. However, CNT17 exhibited a higher complex permittivity than CNT18. This is explained by the RC and fiber volume fraction of the composites. The MWNT weight fraction is defined by the matrix level: even though the MWNT weight fraction was lower, the high RC

Table I. Prepreg Characteristics

Abbreviation	Manufacturing method	Liquid epoxy + MWNT wt %	MWNT wt % in the prepreg resin	R/C
CNT17	Method (a)	YD-128 + 6wt %	1.7	56.3
CNT18	Method (b)	YD-114 + 8wt %	1.8	41.5

Table II. Tensile and Shear Test Results Normalized by the Fiber Volume Fraction

Composites	Tensile modulus (GPa)	Tensile strength (MPa)	Shear modulus (GPa)	Shear strength (MPa)
GEP118	0.484	7.143	0.097	0.841
CNT17	0.612	10.394	0.114	0.897
CNT18	0.571	9.157	0.108	0.939

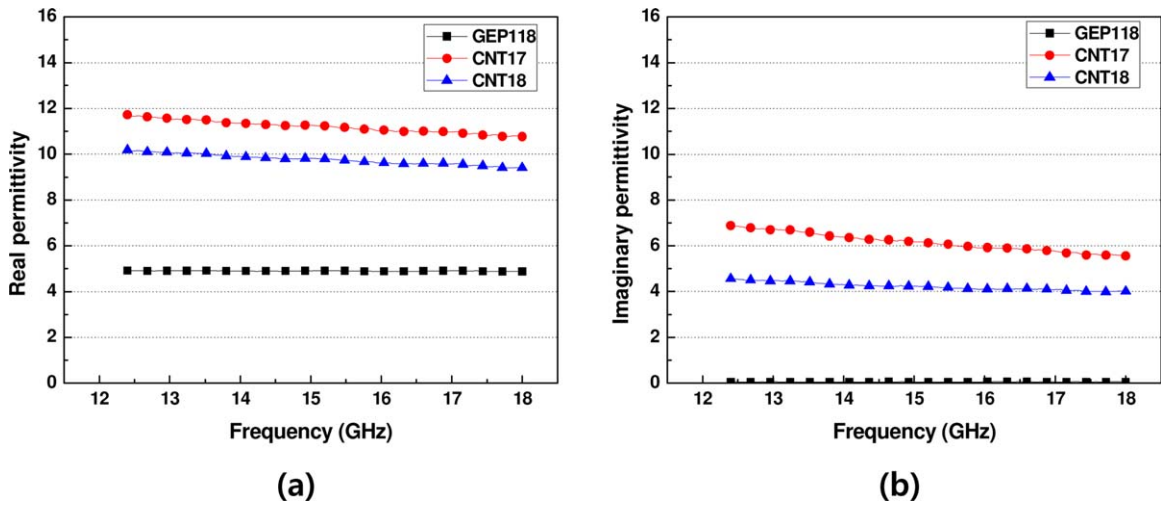

Figure 11. Complex permittivity of the composites: (a) Rear, (b) Imaginary. [Color figure can be viewed in the online issue, which is available at wileyonlinelibrary.com.]

could cause a higher total amount of MWNT. A high RC causes a low fiber volume fraction in the same curing process. Consequently, the MWNT weight fraction of CNT18 was higher than that of CNT17, but the fiber volume fraction of CNT18 was higher than that of CNT17. This caused in the results described in Figure 11.

Single slab absorbers can be designed using the measured complex permittivity and eq. (3). First, RAS was simulated using the commercial software for electromagnetic wave analysis (CST MWS, Computer Simulation Technology). The analysis model was a single slab absorber and perfect electric conductor (PEC), as depicted in Figure 12. The boundary conditions included the tangential electric fields and normal magnetic fluxes being set to zero along the *x*-axis, and the tangential magnetic fields and normal electric fluxes being set to zero along the *y*-axis. The electromagnetic wave was transverse electromagnetic wave (TEM) mode; the waveguide port was in *z*-axis plane and was normal to the *z*-axis. The complex permittivities of the composites were applied in order to analyze the reflection loss of the designed RAS. The simulation was conducted in the Ku-band, from 12 to 18 GHz.

The simulation results using various thicknesses for the CNT17 and CNT18 composites are presented in Figure 13. The difference in the complex permittivity of the CNT17 and CNT18

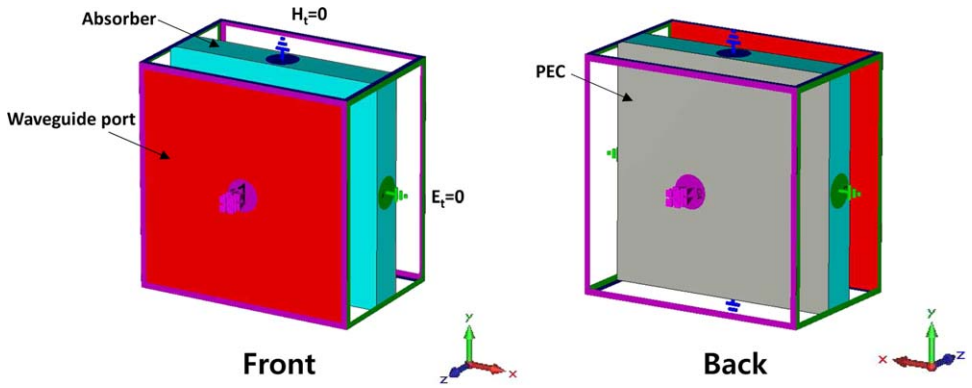

Figure 12. Simulation model in CST MWS. [Color figure can be viewed in the online issue, which is available at wileyonlinelibrary.com.]

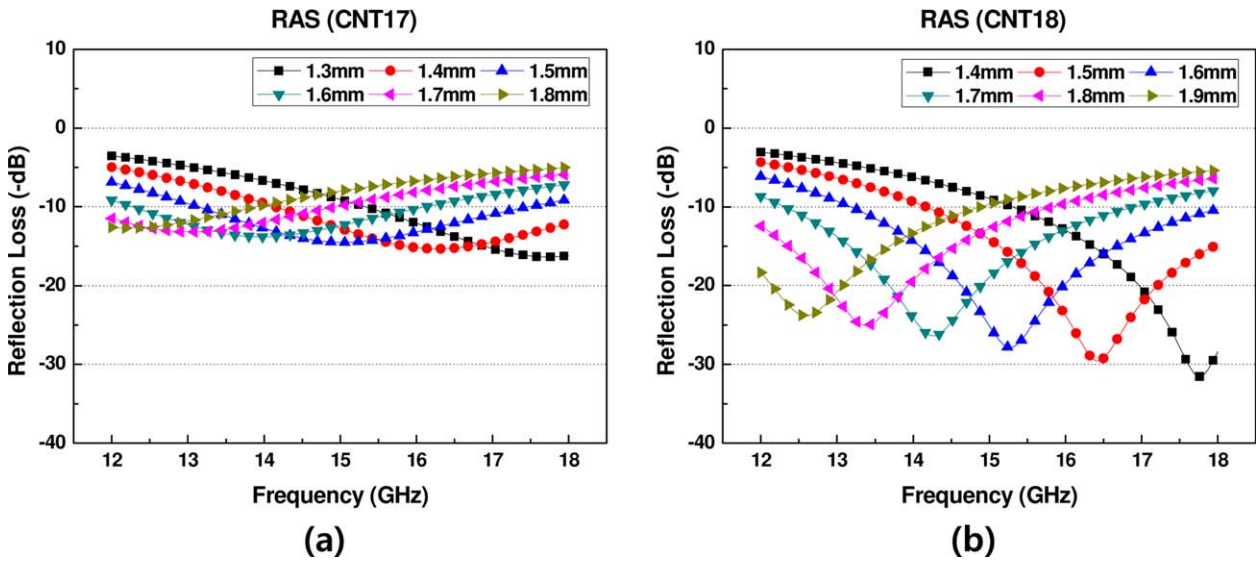

Figure 13. Single slab absorber; (a) CNT17, (b) CNT18. [Color figure can be viewed in the online issue, which is available at wileyonlinelibrary.com.]

composites led to different simulation results, even though the model had the same thickness. It was difficult for the RAS using the CNT17 composite to cover −10 dB bandwidth in the whole Ku-band, and it did not clear resonance peak. The resonance peak was not more than −20 dB. This resulted from the complex permittivity of the CNT17 composite in the Ku-band not close to the solution for eq. (3). The RAS using CNT18 composite exhibited a wider −10 dB bandwidth and a clearer resonance peak than the RAS using CNT17. This indicates that the complex permittivity of CNT18 fits well with eq. (3), although it is not a perfect solution.

The RAS was designed at 15 GHz and it was verified using the CNT18 composite, which exhibited better −10 dB bandwidth and reflection loss. The RAS was designed using an in-house MATLAB code. The designed thickness was 1.62 mm for 15 GHz, and the RAS was manufactured using 12 plies of CNT18. The manufactured RAS thickness was 1.612 mm, and it was difficult to match the designed thickness perfectly because the composite had a fixed thickness per ply. The coaxial line measurement system was used to measure the reflection loss of the RAS with the TEM mode electromagnetic wave, because the waveguide cannot generate a TEM mode electromagnetic wave. The specimen for the coaxial line had a donut shape. Thus, the manufactured RAS was cut into a donut shape with a 7 mm outer diameter and a 3.04 mm inner.

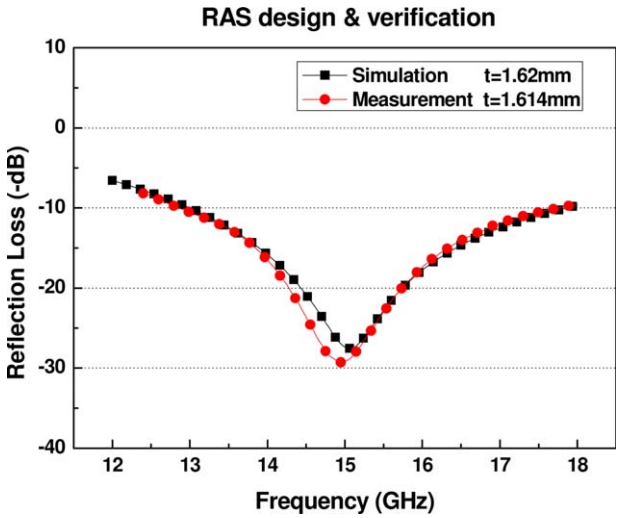

Figure 14. Simulation RAS and verification. [Color figure can be viewed in the online issue, which is available at wileyonlinelibrary.com.]

The simulation and measurement results are presented in Figure 14. The black squares indicate the simulation results and the red circles indicate the measurement result of the RAS. There was a thickness mismatch between the design RAS and specimens for measurement, and the simulation results and measurement result incurred reflection loss difference. The RAS thickness was thinner than the designed thickness, but the resonance peak of the RAS was shifted to a lower frequency. In general, the thickness was thinner and the resonance peak shifted to be higher; these trends are described in Figure 13. The RAS thickness was measured to be thinner than its real thickness. First, the composite used in this research consisted of the woven glass fiber and matrix; also, the peel ply was used when it cured. Therefore, the microsurface bumps and dents can occur. If the thickness was measured at the dented point, it would be thinner. Second, the thickness was measured using a pinhead micrometer, which can push the material. Thus, the thickness could be made thinner during measurement than the actual thickness. Moreover, complex permittivity could have local discrepancies, even though the MWNT was well dispersed.

However, the thickness difference was not significant and the reflection loss trend was well matched. These results demonstrate that the CNT18 manufactured in this research could be used as a RAS in the Ku-band. The RAS −10 dB bandwidth is from 12.87 to 17.78 GHz (4.91 GHz) and the maximum reflection loss occurred at 14.95 GHz and −29.2 dB.

CONCLUSIONS

In this study, a glass fiber composite prepreg was manufactured with the MWNT added epoxy using two different methods. The callendering method was used to disperse the MWNTs uniformly and to resolve the MWNT agglomeration problem. The tensile and shear tests were conducted and the results were compared with a commercial glass fiber composite prepreg (GEP 118). The fiber volume fraction of the CNT18 manufactured using Method (b) was more than 50%, and the tensile and shear properties of CNT18 were not significantly lower than those of the GEP 118. CNT18 is sufficient to replace GEP 118 as a structural material. Next, a single slab electromagnetic wave absorber was designed and simulated using the complex permittivities of CNT17 and CNT18. CNT18 exhibited a wider −10 dB bandwidth from 12.87 to 17.78 GHz (4.91GHz) and stronger reflection loss of −29.2 dB at 14.95 GHz. Finally, a single slab electromagnetic wave absorber was manufactured and verified using CNT18. The measurement results are well matched with the simulation results.

ACKNOWLEDGMENTS

This work was supported by Agency for Defense Development as a part of basic research program under the contract UD130045JD.

REFERENCES

1. Gibson, R. F. Principles of Composite Material Mechanics; Corrigan, J. J.; Castellano, E., Eds.; McGraw-Hill: Singapore, **1994**; Chapter 1, p 1.
2. Campbell, F. C. Manufacturing Technology for Aerospace Structural Materials; Elsevier: Amsterdam, **2006**; Chapter 7, p 273.
3. Panwar, V.; Mehra, R. M.; Park, J. O.; Park, S. H. *J. Appl. Polym. Sci.* **2012**, *125*, 610.
4. Oh, J. H.; Kang, J. H.; Kim, C. G. *Compos. Part B Eng.* **2004**, *35*, 49.
5. Lee, S. E.; Kang, J. H.; Kim, C. G. *Compos. Struct.* **2006**, *76*, 397.
6. Kim, J. B.; Lee, S. K.; Kim, C. G. *Compos. Sci. Technol.* **2008**, *68*, 2909.
7. Shin, J. H. Design and Fabrication of RAS with Carbon Nanoparticles added Kevlar Fiber Reinforced Composite; Master Thesis, Korea Advanced Institute of Science and Technology, Daejeon, Republic of Korea, 2011.
8. Li, Q.; Pang, J.; Wang, B.; Tao, D.; Xu, X.; Sun, L.; Zhai, J. *Adv. Powder. Technol.* **2013**, *24*, 288.
9. Tyagi, S.; Verma, P.; Baskey, H. B.; Agarwala, R. C.; Agarwala, V.; Shami, T. C. *Ceram. Int.* **2012**, *38*, 4561.
10. Kim, M. G.; Hong, J. S.; Kang, S. G.; Kim, C. G. *Compos. A Appl. Sci.* **2008**, *39*, 647.
11. Mazumdar, S. K. Composites Manufacturing: Materials, Product, and Process Engineering; CRC Press: Boca Raton, FL, **2002**; Chapter 2, p 58.
12. Rosca, I. D.; Hoa, S. V. *Carbon* **2009**, *47*, 1958.
13. ASTM D3039 Standard Test Method for Tensile Properties of Polymer Matrix Composite Materials; ASTM International: West Conshohocken, PA, United States, 2008; p 1.
14. ASTM D5397 Standard Test Method for Shear Properties of Composite Materials by the V-Notched Beam Method, ASTM International: West Conshohocken, PA, United States, 2005; p 1.
15. ASTM D3171 Standard Test Method for Constituent Content of Composite Materials, ASTM International: West Conshohocken, PA, United States, 2009; p 1.
16. Vinoy, K. J.; Jha, R. M. Radar Absorbing Materials from Theory to Design and Characterization; Kluwer Academic Publishers: Boston, **1996**; Chapter 4, p 97.